Journal of Rock Mechanics and Geotechnical Engineering 16 (2024) 1140–1152

Contents lists available at ScienceDirect

Journal of Rock Mechanics and Geotechnical Engineering

journal homepage: www.jrmge.cn

Full Length Article

Efficient slope reliability analysis under soil spatial variability using maximum entropy distribution with fractional moments

Chengxin Feng [a,*], Marcos A. Valdebenito [b], Marcin Chwała [c], Kang Liao [d], Matteo Broggi [a], Michael Beer [a,e,f]

[a] Institute for Risk and Reliability, Leibniz University Hannover, Callinstr. 34, Hannover, 30167, Germany
[b] Chair for Reliability Engineering, TU Dortmund University, Leonhard-Euler-Str. 5, Dortmund, 44227, Germany
[c] Faculty of Civil Engineering, Wrocław University of Science and Technology, Wrocław, Poland
[d] Faculty of Geosciences and Environmental Engineering, Southwest Jiaotong University, Chengdu, 610031, China
[e] University of Liverpool, Institute for Risk and Uncertainty, Peach Street, Liverpool, L69 7ZF, United Kingdom
[f] International Joint Research Center for Resilient Infrastructure & International Joint Research Center for Engineering Reliability and Stochastic Mechanics, Tongji University, Shanghai, China

ARTICLE INFO

Article history:
Received 10 February 2023
Received in revised form
22 August 2023
Accepted 4 September 2023
Available online 4 November 2023

Keywords:
Slope
Random field
Reliability analysis
Maximum entropy distribution
Latinized partial stratified sampling

ABSTRACT

Spatial variability of soil properties imposes a challenge for practical analysis and design in geotechnical engineering. The latter is particularly true for slope stability assessment, where the effects of uncertainty are synthesized in the so-called probability of failure. This probability quantifies the reliability of a slope and its numerical calculation is usually quite involved from a numerical viewpoint. In view of this issue, this paper proposes an approach for failure probability assessment based on Latinized partially stratified sampling and maximum entropy distribution with fractional moments. The spatial variability of geotechnical properties is represented by means of random fields and the Karhunen-Loève expansion. Then, failure probabilities are estimated employing maximum entropy distribution with fractional moments. The application of the proposed approach is examined with two examples: a case study of an undrained slope and a case study of a slope with cross-correlated random fields of strength parameters under a drained slope. The results show that the proposed approach has excellent accuracy and high efficiency, and it can be applied straightforwardly to similar geotechnical engineering problems.
© 2024 Institute of Rock and Soil Mechanics, Chinese Academy of Sciences. Production and hosting by Elsevier B.V. This is an open access article under the CC BY-NC-ND license (http://creativecommons.org/licenses/by-nc-nd/4.0/).

1. Introduction

Geotechnical engineering must confront different sources of uncertainty, which can be suitably described by random fields (Phoon and Kulhawy, 1999; Sudret and Der Kiureghian, 2000; Baecher, 2023). Therefore, in recent years, random field theory has been commonly used to describe spatial variability of natural soils (Griffiths et al., 2011; Zhao and Wang, 2020; Han et al., 2022; Jiang et al., 2022). For example, Ji et al. (2018) estimated the failure probability (P_f) of a slope by the first-order reliability method (FORM). Jiang et al. (2015) developed an efficient reliability analysis approach based on multiple stochastic response surfaces. Li and Wang (2022) developed an efficient active learning reliability analysis method using adaptive Bayesian compressive sensing and Monte Carlo simulation (MCS). Wang et al. (2011) performed a reliability analysis approach for slope stability problems using subset simulation. The main methods for the propagation of uncertainty are direct MCSs, approximation methods, surrogate model methods, and sampling methods (Jiang et al., 2022; Kumar and Tiwari, 2022). The direct MCS is often used to face engineering problems with a high probability of failure (10^{-1}–10^{-3}) due to its high accuracy (Cho, 2010). By surveying engineers involved in slope stability analysis, an effort was made to determine an acceptable probability of failure for slopes by Santamarina et al. (1992). The results of this survey can be seen in Table 1. Accordingly, low failure probabilities for slopes are expected in several different practical applications (Salgado and Kim, 2014). It should be noted that there are already several studies on geotechnical engineering that involve a low probability of failure considering spatial variability (Jiang et al., 2022). In fact, surrogate models perform very well in terms of efficiency and accuracy for calculating

* Corresponding author.
E-mail address: feng.chengxin@irz.uni-hannover.de (C. Feng).
Peer review under responsibility of Institute of Rock and Soil Mechanics, Chinese Academy of Sciences.

https://doi.org/10.1016/j.jrmge.2023.09.006
1674-7755 © 2024 Institute of Rock and Soil Mechanics, Chinese Academy of Sciences. Production and hosting by Elsevier B.V. This is an open access article under the CC BY-NC-ND license (http://creativecommons.org/licenses/by-nc-nd/4.0/).

Table 1
Acceptable failure probability of slopes (Santamarina et al., 1992).

Condition	Acceptable P_f
Temporary structures: no potential life loss	10^{-1}
Existing large cut on interstate highway	10^{-2}
Lives may be lost when slopes fail	10^{-3}
Acceptable for all slopes	10^{-4}
Unnecessarily low	$<10^{-5}$

the reliability of slopes in view of spatial variability. Still, there is a limitation regarding the underlying dimensionality of the problem at hand (Müller et al., 2013). To overcome such limitations, advanced simulation methods have been developed because of their improved accuracy, efficiency, and robustness with respect to dimensionality (Li et al., 2016a; Wang et al., 2020).

The classical MCS method is based on the calculation of a large number of random samples to obtain the failure probability. The results obtained with increasing sampling converge to the precise results (Metropolis and Ulam, 1949; Rubinstein and Kroese, 2016). However, it is challenging to calculate a low probability of failure ($<10^{-4}$) by means of simulation (Wang et al., 2011). For estimating failure probabilities in the order of 10^{-2} with sufficient accuracy, the MCS method needs to perform about 2000 sets of samples. Latin hypercube sampling may help in reducing variance to improve the quality of the estimates. In fact, it is perhaps one of the most widely used random sampling methods for uncertainty quantification and reliability analysis (Helton and Davis, 2003). However, Latin hypercube needs to generate a significant number of samples to calculate small failure probabilities, just like plain Monte Carlo. Therefore, many scholars have conducted a number of studies on efficient sampling methods. Partially stratified sampling (PSS) is an improved method that combines the advantages of stratified sampling and Latin hypercube sampling (Shields and Zhang, 2016). Stratified sampling is a method in which the sampling range is divided into different strata according to specific rules. Then samples are obtained independently and randomly from the different strata, while each dimension in the space of random variables is stratified. Thus, PSS has been widely spread because of its excellent properties. Nevertheless, some problems, such as ensuring the best subspace decomposition, have not been fully solved. Therefore, the Latinized partially stratified sampling (LPSS) has been proposed in the literature as a solution for the difficulties related to using the PSS methods (Shields and Zhang, 2016).

Another challenge associated with reliability analysis is estimating the probability density function associated with a response of interest based on samples. A feasible approach to characterize such probability density function is to evaluate the information about its moments, such as the mean and variance. Then, one can approximate the sought distribution by means of the classical maximum entropy distribution, which is the most likely distribution among various distributions available (Jaynes, 1957; Kapur and Kesavan, 1992). Although conceptually feasible, there are still several difficulties associated with the maximum entropy distribution, such as the relatively large number of moments required to achieve reasonable accuracy in modeling the tail of the distribution (Tagliani, 1999; Zhang and Pandey, 2013). With the rise of fractional order moments and the fact that a finite number of fractional moments can be used to characterize the distribution of a random variable, the maximum entropy distribution has been applied extensively in the last few years (Zhang et al., 2019, 2020). Indeed, Xu and Dang (2019) tackled high-dimensional reliability problems using the fractional moments-based maximum entropy method. Furthermore, Deng (2022) proposed an objective and unbiased method to estimate probability distributions of a soil property using the maximum entropy method from fractional moments of observed data. All of the aforementioned contributions suggest that the maximum entropy distribution method based on fractional moments is very effective, particularly for high-dimensional reliability analysis.

According to the above paragraphs, calculating small failure probabilities associated with slope stability problems is crucial. There is no unified and efficient method to deal with this issue up to the present time. Therefore, in this paper, LPSS is employed to estimate the failure probability of slopes considering spatial variability using the maximum entropy distribution with fractional moments (MEDFM). Firstly, the autocorrelation function is considered to describe the spatial variability of geotechnical materials, which is applied in conjunction with the Karhunen-Loève (K-L) expansion to characterize soil properties through random fields. The advantages of LPSS and the basics of MEDFM are presented next. Then the specific implementation procedures of the present approach based on LPSS and MEDFM are described. Finally, the proposed approach is used to analyze a case study of an undrained slope and a case study of a slope with cross-correlated random fields of strength parameters.

The paper is structured as follows. Section 2 describes the basic methodology used in this paper, comprising random field modeling, LPSS and MEDFM. The implementation procedure of the proposed LPSS-MEDFM approach is presented in Section 3. Section 4 verifies the effectiveness of the proposed approach using two slopes as examples. The last section presents some of the conclusions of this paper.

2. Methodology

2.1. Random field model

In recent years, random fields have become a commonly used approach to represent the spatial variability of soil parameters, whose application demands to determine random field parameters such as distribution type, autocorrelation function, autocorrelation distance, etc. For this reason, many scholars have been working on this subject in recent years, such as fitting the real distribution of geotechnical parameters with the maximum entropy distribution method (Wang and Jiang, 2023), solutions considering in situ testing data, such as conditional random field, Bayesian inference, etc (Li et al., 2016b; Wang et al., 2016), or determination of the autocorrelation function and autocorrelation distance (Cami et al., 2020). Among the many methods available, we use the K-L expansion method to generate random fields in this study. This is because K-L expansion is optimal among series expansion methods in the global mean square error concerning the number of random variables in the representation (Dai et al., 2019).

2.1.1. Log-normal random fields

The autocorrelation function is critical in expressing the properties of the random field (Ching et al., 2019). Some of the most commonly used autocorrelation functions are single exponential and square exponential autocorrelation functions. In particular, the single exponential autocorrelation function is used in this paper to compare the results with previous works:

$$\gamma(u,u',v,v') = \exp\left(-\frac{|u-u'|}{l_h}-\frac{|v-v'|}{l_v}\right) \tag{1}$$

where $\gamma(u,u',v,v')$ is the single exponential autocorrelation function, (u,v) and (u',v') denote the coordinates of two points in a two-

dimensional (2D) space, exp (·) is the exponential function, l_h is the horizontal correlation distance, l_v is the vertical correlation distance, and |·| denotes the absolute value. Note that the application of the exponential autocorrelation function presented in Eq. (1) has been discouraged in the literature (e.g. Spanos et al., 2007; Faes et al., 2022). However, this autocorrelation function is considered herein as it has been used in the past for several different studies and thus, it is useful for comparisons.

The log-normal random field is a random function defined over a domain where the function's logarithm is a Gaussian random field. It is one of the most common means for modeling uncertainty in soil properties, and as such, it is considered within this work. Therefore, in this subsection, essential aspects related with these fields are discussed. It should be noted that this paper considers weakly stationary log-normal random fields. There are many ways to represent random fields, in which the K-L expansion is widely used due to its fast convergence property (Cho, 2010). The log-normal random field can be expressed as

$$\psi(\boldsymbol{x}) = \exp\left(\mu_g + \sigma_g \sum_{j=1}^{n} g_j(\boldsymbol{x})\zeta_j\right) \tag{2}$$

where $\psi(\boldsymbol{x})$ is the realization of the log-normal random field, $g_j(\boldsymbol{x})$ is the basis functions, ζ_j denotes the standard Gaussian random variable, n is the order of truncation of the K-L expansion, and $\boldsymbol{x} = [u,v]$ is the vector of 2D coordinates. The parameters μ_g and σ_g represent the mean and standard deviation of the underlying Gaussian field that is associated with the log-normal random field. The mean μ and standard deviation σ of the weakly stationary log-normal random field are related with μ_g and σ_g through the following expressions:

$$\mu_g = \ln\left(\frac{\mu^2}{\sqrt{\mu^2+\sigma^2}}\right) \tag{3}$$

$$\sigma_g = \sqrt{\ln\left[1+(\sigma/\mu)^2\right]} \tag{4}$$

The basis function $g_j(\boldsymbol{x})$ takes the following form:

$$g_j(\boldsymbol{x}) = \sqrt{\lambda_j} f_j(\boldsymbol{x}) \tag{5}$$

where λ_j and f_j denote the j-th eigenvalue and j-th eigenfunction associated with the autocorrelation function. They are obtained by solving the homogeneous Fredholm equation of the second type, which is

$$\int_{\Omega} \gamma_G(u,u',v,v') f_j(u',v')\mathrm{d}u'\mathrm{d}v' = \lambda_j f_j(u,v) \tag{6}$$

where Ω is the spatial domain; and γ_G is the autocorrelation function of the underlying Gaussian process, which is equal to

$$\gamma_G(u,u',v,v') = \frac{1}{\sigma_g^2}\ln\left(\frac{\sigma^2\gamma(u,u',v,v')}{\mu^2}+1\right) \tag{7}$$

The error of K-L expansion associated with the underlying Gaussian field is

$$\varepsilon_t(\psi(\boldsymbol{x})) = 1 - \frac{\sum_{j=1}^{n}\lambda_j}{\sum_{j=1}^{+\infty}\lambda_j} \tag{8}$$

where $\varepsilon_t \in [0,1)$ is the error of the n-term expansions of the random field. Clearly, the error tends to become smaller as the number of terms n included in the K-L expansion becomes larger.

2.1.2. Cross-correlated log-normal random fields

Random field models of multiple parameters are often required in geotechnical engineering practice. Moreover, cross-correlations between two (or more) geotechnical parameters may exist, as discussed in the literature. In fact, the cohesion c and the friction angle φ are usually employed for slope reliability analysis and are considered as negatively correlated. As this is precisely the topic of this contribution, the cross-correlation between the random fields models for cohesion and the friction angle is addressed in this subsection following the approach proposed in Vořechovskỳ (2008) and Sepúlveda-García and Alvarez (2022).

The cohesion and friction angle are modeled as weakly-stationary log-normal random fields. The mean values and standard deviations for each of these two fields are denoted as (μ_c, σ_c) and $(\mu_\varphi, \sigma_\varphi)$, respectively. It is assumed that both random fields share the same exponential correlation function shown in Eq. (1). This is reasonable because spatial correlation is caused by the variation of soil properties over space. Therefore, the decomposition of a given autocorrelation function is performed only once. Furthermore, it is assumed that the cross-correlation between the two random fields is equal to ϱ. Thus, following Vořechovskỳ (2008), these two random fields can be represented using the K-L expansion, i.e.

$$\psi_c(\boldsymbol{x}) = \exp\left(\mu_{g,c} + \sigma_{g,c}\sum_{j=1}^{n}\sqrt{\lambda_j} f_j(\boldsymbol{x})\xi_j^c\right) \tag{9}$$

$$\psi_\varphi(\boldsymbol{x}) = \exp\left(\mu_{g,\varphi} + \sigma_{g,\varphi}\sum_{j=1}^{n}\sqrt{\lambda_j} f_j(\boldsymbol{x})\xi_j^\varphi\right) \tag{10}$$

where ξ_j^c and ξ_j^φ denote a set of Gaussian random variables, $\mu_{g,c}$ and $\sigma_{g,c}$ are the mean and standard deviation of the underlying Gaussian random field associated with cohesion c, and $\mu_{g,\varphi}$ and $\sigma_{g,\varphi}$ are the mean and standard deviation of the underlying Gaussian random field associated with the friction angle φ. Note that $(\mu_{g,c}, \sigma_{g,c})$ and $(\mu_{g,\varphi}, \sigma_{g,\varphi})$ are calculated based on (μ_c, σ_c) and $(\mu_\varphi, \sigma_\varphi)$ by means of Eqs. (3) and (4), respectively.

The random variables ξ_j^c and ξ_j^φ $(j = 1,\ldots,n)$ possess zero mean, unit standard deviation and exhibit a correlation structure. The latter is required in order to ensure that the cross-correlation between random fields is equal to ϱ. In order to generate samples of these random variables, the following procedure is followed (Vořechovskỳ, 2008). First, the correlation coefficient ρ associated with the cross-correlation of two log-normal random fields is projected to obtain the equivalent cross-correlation ϱ_g between two underlying Gaussian fields through the expression (Liu and Der Kiureghian, 1986):

$$\varrho_g = \frac{\ln[1+\varrho(\sigma_c/\mu_c)(\sigma_\varphi/\mu_\varphi)]}{\sigma_{g,c}\sigma_{g,\varphi}} \tag{11}$$

Then, the correlation matrix $\boldsymbol{D}$ between the two underlying Gaussian random fields is established as

$$\boldsymbol{D} = \begin{bmatrix} \boldsymbol{I} & \varrho_g \boldsymbol{I} \\ \varrho_g \boldsymbol{I} & \boldsymbol{I} \end{bmatrix} \tag{12}$$

where $\boldsymbol{I}$ is the unit matrix of order n and D possesses dimension $2n \times 2n$ and ϱ_g are the elements of the cross-correlation matrix. After the matrix $\boldsymbol{D}$ is determined, its eigenvalues Λ^D and eigenvectors Φ^D can be calculated according to the following expression:

$$\boldsymbol{D}\Phi^D = \Phi^D \Lambda^D \tag{13}$$

The eigenvalue needs to be sorted after the calculation ($\lambda_1^D \geq \lambda_2^D \geq \lambda_3^D I \geq \ldots \geq \lambda_{2n}^D$). Afterwards, it is possible to simulate the required random variables ξ_j^c and ξ_j^φ ($j = 1, \ldots, n$) by means of the following expression:

$$\xi^D = \Phi^D \left(\Lambda^D\right)^{1/2} \varsigma \tag{14}$$

where ς is a realization of a standard Gaussian distribution with independent components of dimension $2n$ and $\xi^D = [\xi_1^c, \ldots, \xi_n^c, \xi_1^\varphi, \ldots, \xi_n^\varphi]$.

2.2. Sampling strategy

2.2.1. Stratified sampling and partially stratified sampling

Standard stratified sampling (SS) is a method for generating stratified samples for all dimensions involved in a problem. It divides the sampling space into strata according to a certain characteristic or a specific rule and then draws samples independently and randomly from each strata. The major challenge of SS is that it may require a large number of strata and samples for high-dimensional problems. This is due to the fact that it is not easy to stratify all dimensions simultaneously in a high-dimensional sample space. PSS method can be seen as the generalization of SS (Shields and Zhang, 2016). In essence, PSS applies SS to sampling subspaces. It means that the random variables of a problem are grouped into different subspaces and SS is applied only to those subspaces. Fig. 1a and b provides schematic illustrations of SS and PSS, respectively. Fig. 1a shows the standard SS in the space of two random variables, where four strata and four samples are considered. Fig. 1b represents PSS applied to a problem that involves four random variables grouped into two sample subspaces. The first subspace groups random variables ξ_1 and ξ_2 while the second subspace groups random variables ξ_3 and ξ_4, respectively. Then, according to the standard stratified sampling method, low-dimensional random samples are generated within each stratum belonging to a subspace. The low-dimensional samples generated in each subspace are randomly grouped to obtain the complete n-dimensional samples. This last step is represented in Fig. 1b with arrows. Compared to the standard SS method, PSS has the advantage of being applicable to high-dimensional sample spaces. The main challenge of PSS is to select which random variables should be paired in the subspace. Preferably, random variables which exhibit strong interaction over the output of a numerical model should be paired together. However, determining a priori which variables interact can be challenging for cases of practical interest.

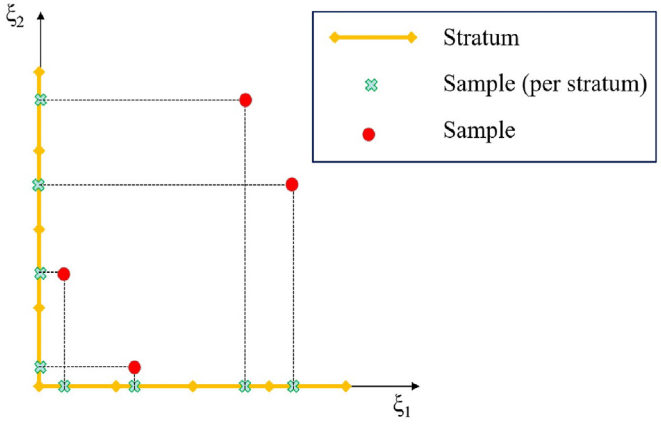

Fig. 2. Diagram of the LHS.

2.2.2. Latin hypercube sampling

Latin hypercube sampling (LHS) is a method for conducting random sampling from multivariate parameter distributions (Helton and Davis, 2003). LHS stratifies the sample space associated

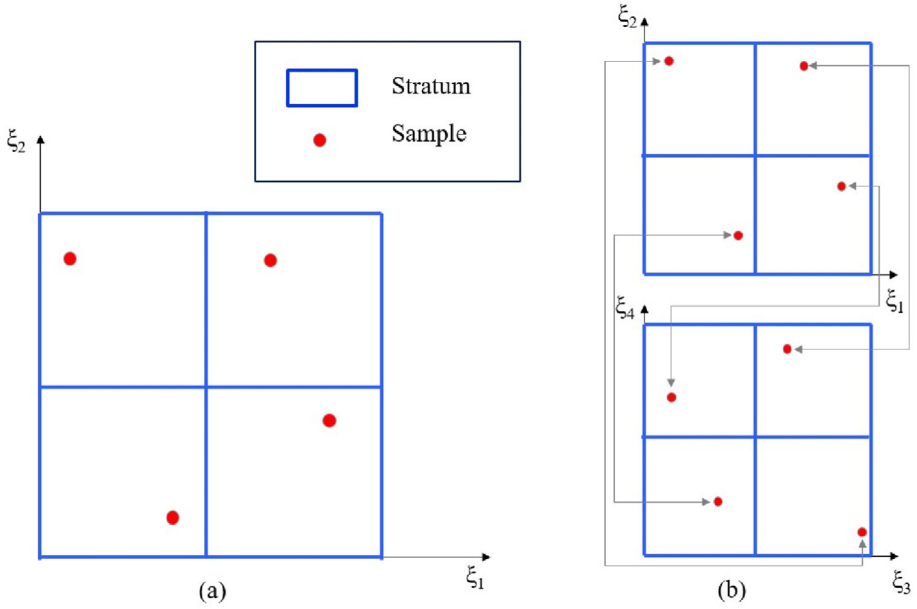

Fig. 1. Diagrams of (a) SS and (b) PSS.

with each random variable individually. This constitutes a major difference with stratified sampling, where the sampling space associated with all random variables is stratified at once. LHS is well suited for capturing additive effects of the input random variables on the output of a numerical model and thus, it has been widely used in recent years (Shields, 2016). Fig. 2 shows the schematic diagram of LHS. In this figure, the yellow line represents the stratum, the green symbol represents the randomly selected samples in the strata, and the red points represent the samples generated by LHS by random pairing.

2.2.3. Latinized partially stratified sampling

LPSS combines the features of stratified sampling, PSS and Latin hypercube sampling. Conceptually, LPSS can be divided into three steps. The first step is to divide the possibly high-dimensional sample space into subspaces using PSS. Random variables are paired in subspaces according to appropriate criteria. The second step is to generate samples with Latinized stratified sampling (LSS) in each generated subspace. LSS consists of generating a set of samples that satisfy simultaneously the characteristics of the SS in addition to the characteristics of the LHS. Fig. 3 provides a schematic diagram for generating LSS samples in a 2D subspace, where the objective is to generate a total of four samples. In this figure, the blue lines represent the stratified sampling subspace, and the yellow line represents the stratification of LHS for each random variable. The green symbol represents the samples in each strata of LHS, and the red dots represent the samples in the subspace, which are generated by pairing the samples associated with each random variable within this subspace. It is readily observed from Fig. 3 that the resulting samples fulfill the conditions associated with both stratified and Latin hypercube sampling. The third and final steps of LPSS consist of generating samples by randomly combining the subspace samples generated by LSS.

The main advantage of LPSS over PSS is as follows. Each subspace is sampled using LSS, which means that those samples fulfill the conditions of SS and LHS. In other words, it is possible to capture both interaction and additive effects of the input random variables on the output of a numerical model. Such a strategy can be quite effective in mitigating poor pairing of random variables in a subspace. Therefore, as discussed in SS (Shields and Zhang, 2016), LPSS can effectively combine the best features of both stratified and Latin hypercube sampling.

When using LPSS, it is crucial to determine the subspaces and the number of dimensions in each subspace. The optimal subspaces of LPSS can be determined by means of the calculation of the Sobol' indices of the interaction effects. Previous studies concentrated on the calculation of the Sobol' indices to estimate the interaction effects of random variables in determining the LPSS subspaces (e.g. Shi et al., 2018). However, this approach is limited to rigorously evaluating only interactions in a lower dimensional random space, i.e. up to 6 dimensions in the aforementioned work. On the other hand, in this work, a highly dimensional random input space is taken into account. This is because a high number of random variables are required to accurately represent random fields. Because of this, a considerable computational effort renders unfeasible the employment of Sobol' indices to accurately identify the optimal pair of random variables and LPSS layers. Thus, the pairs are identified by means of a trial approach. However, this trial approach is not detrimental to the method. As a matter of fact, according to Shields and Zhang (2016), '*in LPSS, it is sufficient to stratify a set of variables together simply based on the possibility that they may interact*'. Thus, as a consequence from the findings in the aforementioned work, wrong pairing will not bring any harm and successful pairing will enable better estimation of the sought quantities of interest.

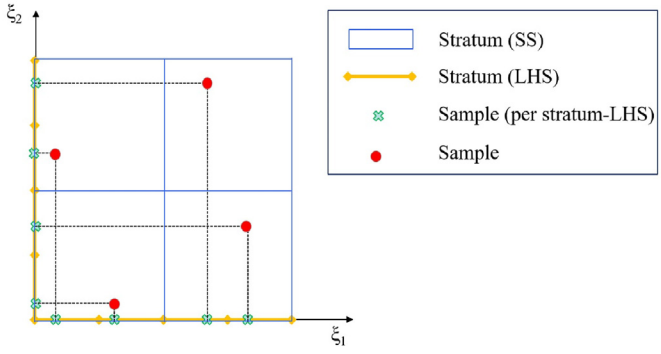

Fig. 3. Diagram of the LPSS.

2.3. Maximum entropy distribution with fractional moments

2.3.1. Maximum entropy distribution

The probability distributions of random variables are usually difficult to obtain, while information about their moments is usually easy to obtain. The probability distribution function of a variable can be approximated by equating the moments of the random variable with the moments of the distribution. It can be found that there are multiple distributions whose moments agree with the moments of measurement of these values, one of which has the maximum entropy. In fact, the maximum entropy distribution is actually the most probable distribution. This is because, in the case of insufficient data, the inferred distribution must coincide with the known data while making the fewest assumptions about the unknown. Moreover, theoretically, the maximum entropy probability distribution based on the given moments has the property of minimum error. Therefore, the maximum entropy distribution is widely used in different problems, such as wind engineering (Pandey, 2002), hydrology (Pandey et al., 2001), Geotechnical engineering (Deng, 2022), etc. Its good results show that it is indeed an excellent method to deal with ill-posed problems. In this paper, the maximum entropy distribution is used to determine the probability distribution function associated with the safety factor that is considered to calculate the failure probability of slopes.

2.3.2. Fractional order moments

The maximum entropy distribution still has some obstacles that prevent its practical implementation, despite its many advantages. A considerable number of moments are essential to accurately characterize the tails of the maximum entropy probability distribution, but in practice only a limited number of sample moments are available (Winterstein and Kashef, 2000). As the number of required moments increases, the problem of moments of the maximum entropy probability distribution becomes pathological, and the tails exhibit oscillatory behavior. Reasonable estimates of the distribution's tails are necessary but challenging because the sample size is usually finite. If the distribution type is known or can be assumed, then the distribution parameters can be estimated by several methods. Unfortunately, in many cases, the functional form of the probability distribution is unknown. If the chosen model is too simple with respect to the number of free parameters or incompatible with the data, the bias error can be significant. Research in recent years has found that fractional-order models can more accurately describe natural physical systems (Zhang and Pandey, 2013). Fractional order moments are a natural generalization of integer order moments. Thus, the sample estimate of the fractional moment associated with a random variable X is

$$\boldsymbol{E}X^{\alpha_m} = \frac{X_1^{\alpha_m} + X_2^{\alpha_m} + \cdots + X_N^{\alpha_m}}{N} \tag{15}$$

where α_m is a real number; N is the number of the samples; and X_1, X_2, …, X_N are the samples of X. It can be calculated in a similar way to the integer moments. The main advantage of fractional moments is their lower sampling variability compared to that of integer-order moments. Moreover, a single low-order fractional-order moment contains information about many central moments. Thus, a finite number of fractional-order moments is sufficient to recover the probability density function. In addition, the use of fractional-order moments can accurately characterize distribution tails.

2.3.3. Construction of maximum entropy distribution

Generating an unknown probability density function from a finite number of integer-order moments is an ill-posed problem. This problem can be solved by using fractional moments because fractional moments contain more probability information than integer-order moments (Zhang et al., 2020). Therefore, in this subsection, fractional order moments are used as constraints to derive probability density functions for high-dimensional reliability analysis using the maximum entropy distribution based on fractional order moments. The entropy is first defined and is denoted as

$$H(f_X) = -\int f_X(x)\ln f_X(x)\mathrm{d}x \tag{16}$$

where $f_X(x)$ is the probability density function (PDF) of a continuous random variable X. The integration domain corresponds to the feasible range of the random variable X.

The form of the maximum entropy distribution obtained using the Euler-Lagrange equation is written as

$$f_X(x) = \exp\left[-\kappa_0 - \sum_{m=1}^{M}\kappa_m(x-b)^{\alpha_m}\right] \tag{17}$$

where b is a location parameter, M is the number of fractional moment constraints, α_m is a real number representing the m-th fractional moment considered, κ_m is the m-th Lagrange's multiplier, and exp $(\cdot)$ is the exponential function. Parameters α_m, M, b and κ_m are selected according to an optimization strategy with respect to a certain objective function described in detail below (see Eq. (20)). Note that M is a positive integer, α_m is a real number, and κ_m is another real number related to the value of α_m. In this paper, the values of M range from 1 to 6, and the values of α_m range from −4 to 4. Numerical validation indicates that these ranges of values for M and α_m are appropriate within the context of the applications studied in this contribution. The process for identifying the aforementioned parameters proceeds as follows. The value of M is first chosen, then the values of the remaining parameters are obtained using an optimization algorithm. Then, the results for different values of M are compared to determine the optimal M according to the principle of minimizing the objective function. The difference from the standard maximum entropy distribution is that α_m is a real number rather than an integer. The rules for its calculation are the same. The normalization constant κ_0 is given as follows:

$$\kappa_0 = \ln\int_b^{+\infty}\exp\left[-\sum_{m=1}^{M}\kappa_m(x-b)^{\alpha_m}\right]\mathrm{d}x \tag{18}$$

Maximum likelihood estimation is used to estimate the model parameters of MED. The likelihood function of Eq. (17) is defined as

$$L(\alpha,\kappa|x) = \prod_{n=1}^{N}\exp\left[-\kappa_0 - \sum_{m=1}^{M}\kappa_m(x_n-b)^{\alpha_m}\right] \tag{19}$$

where x_n is the safety factor f_s calculated from the LPSS samples, and N is the sample size associated with LPSS as explained in Section 2.2. According to the principle of maximum entropy distribution, the maximum value of the likelihood function needs to be identified. The problem of calculating the maximum entropy can be converted into an unconstrained minimization problem. It is important to note that fractional moments are only defined in the positive domain, which means that $x-b$ must be positive. Therefore, the domain of x is defined from b to positive infinity (Zhang et al., 2020). The objective function for identifying this optimal minimum is expressed as

$$Q(\alpha,\kappa,b,M) = \kappa_0 + \sum_{m=1}^{M}\kappa_m E(X-b)^{\alpha_m} + \frac{2M+1}{N} \tag{20}$$

where N is the size of the sample data to be post-processed, and X is the sample datum.

MEDFM can characterize the maximum entropy distribution using information from small amounts of fractional moments. However, the optimization problem is challenging to solve efficiently because the objective function is nonconvex and discontinuous. Heuristic optimization algorithms can find globally optimal solutions that cannot be achieved using traditional methods because they do not require the derivatives of the objective function. In this paper, Genetic algorithms are adopted because they are robust for finding fractional-order global optimal solutions (Whitley, 1994). The Genetic algorithm follows a set of steps, which starts with an initial population of individuals. The algorithm selects the most fit individuals as parents using a selection operator and then generates new offsprings using a crossover operator. The offsprings are then subjected to a mutation operator to introduce some level of randomness to avoid getting stuck in local optimal solutions. Finally, the offsprings are added to the population and updated through a replacement strategy. This process is repeated over multiple generations until the optimal solution is found. The fractional order of MEDFM can be obtained according to the steps of the Genetic algorithm. It is important to note that the result of the fractional order is always different for different cases because it is optimized according to the Genetic algorithm and the latter possesses a random component. Nonetheless, practical numerical experience indicates that differences between parameters identified with independent runs of Genetic algorithms are minimal. Finally, the failure probability can be obtained from the PDF, which also allows to calculate the cumulative distribution function (CDF).

3. Implementation procedure

This section presents the procedure of an efficient approach for the reliability calculation of slopes, as shown in Fig. 4. This approach is flexible because the deterministic computation is decoupled from the stochastic analysis. Therefore, different deterministic methods can be used for the analysis. This procedure consists of seven main steps as follows:

(1) When a random field is used to characterize the spatial variability of the soil, the first step is to determine the type of autocorrelation function. The correlation of soils at different locations in the space needs to be considered. The selection of different autocorrelation functions and their parameters significantly impacts the probability of failure, so it should be

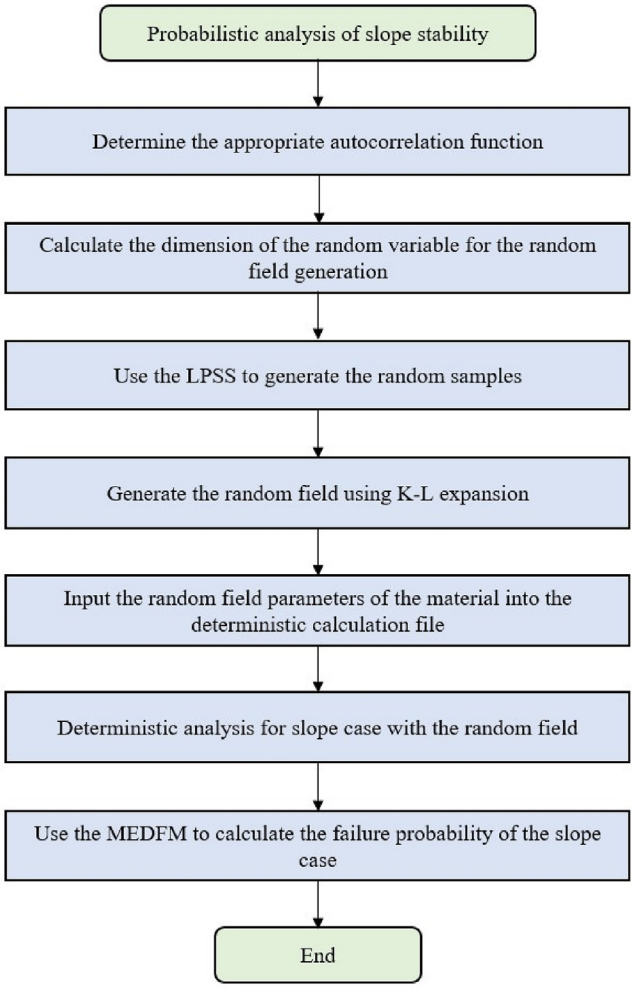

Fig. 4. Flowchart of the proposed approach.

chosen reasonably. In this paper, a single exponential autocorrelation function is used to generate the random field for comparison with existing examples.

(2) The second step is to generate the random field. In this paper, the K-L expansion method is used. The error resulting from the random field generated by K-L is calculated according to the error equation of the random field. An accuracy of 95% is enough for most engineering scenarios when generating the random field. Therefore, the number of K-L expansion terms required to generate the random field is determined based on its 95% accuracy. In this paper, a random field requires 80 K-L expansion terms, i.e. an 80-dimensional random variable space is required to generate a random field.

(3) The third step is to generate samples of the random variables associated with the description of the random field. These samples are generated following the LPSS method. The dimensionality of the random variable needs to be determined by the number of expansion terms in the random field. The specific steps of LPSS are described in detail in Section 2.2. According to the analysis in the previous step, generating a random field requires an 80-dimensional random variable. This means that when we consider two correlated random fields, 160-dimensional random variables are considered. The specific number of samples to implement the proposed approach was determined based on specific cases. For the large failure probability ($>10^{-3}$) of example 1, at least 900 samples are required to obtain reliable results. For small failure probability (10^{-3}–10^{-5}) of example 2, at least 3600 samples are required to obtain reliable results.

(4) Samples of the random field are generated according to the K-L expansion method in this step. In this paper, a discrete approach is used to generate random fields. Specifically, the centre points of the mesh are used as discrete points. The problem of random field expansion is first converted into a problem of the second type of integral equation. Then the eigenvalues and eigenvectors of the covariance function are solved. Finally, the random variables are multiplied by the eigenvalues and eigenvectors to obtain the random field. For the case of the undrained slope in the first example, the random field of the shear strength parameter only needs to be considered. For the case of the c-φ slope in the second example, the c and φ are considered to generate cross-correlated random fields.

(5) The generated material parameters of the random field are brought into the calculation file associated with the numerical solution of the slope stability problem according to their corresponding position. In this step, the emphasis is on assigning material parameters to specific locations in the geometric model. A MATLAB program is used to input the random field material parameters into the finite element calculation file. In this work, we have used GeoStudio software for solving finite element method (FEM) models.

(6) The safety factor f_s is calculated for slopes considering the samples of the random fields. In this step, calculations can be performed with commercial software for geotechnical engineering or in-house code. The solver is called to perform calculations on the finite element calculation file with the samples of material parameters of the random field. After each calculation, a MATLAB program extracts f_s from the output results file.

(7) The last step is to use MEDFM to calculate the failure probability of the slope. The fractional order moments of f_s are calculated with the samples generated in the previous step, and then the PDF and CDF of f_s are fitted according to the maximum entropy distribution method. Then the probability that f_s is less than 1, which is the failure probability of the slope, is obtained according to the CDF. The specific steps of MEDFM are described in detail in Section 2.3.

In this work, the number of samples generated with LPSS needs special consideration. The minimum value of the required samples can be determined depending on the value of the failure probability. For real cases, the exact number of calculations needs to be determined based on the results of the analysis.

4. Examples

In this section, two examples are given to illustrate the efficiency and accuracy of the presented approach. For this purpose, the K-L method was implemented using MATLAB to simulate the random field. Furthermore, GeoStudio was used for the deterministic finite element analysis. In addition, a routine for MATLAB was developed to perform LPSS. Finally, the MEDFM is coupled with the LPSS to analyze the slope reliability.

4.1. Example 1: application to a saturated clay slope

For comparison purposes, the undrained clay slope studied by Jiang et al. (2014) and Cho (2010) is investigated in the first

example. The geometry of the scenario considered is given in Fig. 5. The total slope height in this example is 10 m, and the length is 30 m. In the analysis, only the cohesive force is considered as a random field, while the angle of internal friction is assumed to be 0. The mesh types are 4-node quadrilateral meshes and 3-node triangular meshes. Most of the finite elements are square, and some degenerate into triangles. In Fig. 5, the finite element mesh consists of 910 elements and 981 nodes. For illustrative purposes, a conventional elastic and perfect plastic model based on the Mohr-Coulomb failure criterion is used to represent the stress-strain behavior of the soil. The boundary conditions are fully fixed on the vertical ends of the bottom and left sides of the model.

Undrained shear strength cohesion is considered a random field with a log-normal distribution. Table 2 summarizes the statistical properties of the soil parameters for the slope considered. Young's modulus, Poisson's ratio, and the soil unit weight in this example are considered deterministic quantities because their influence is relatively small compared to cohesion. Based on the average value of the undrained shear strength, a minimum slope f_s of 1.366 was obtained using a finite element method based on a critical surface search algorithm, which is implemented in SIGMA/W and SLOPE/W. For comparison, the safety factor of this slope model using the limit equilibrium method was also calculated. The f_s is 1.354 using the Morgenstern-Price method, which is consistent with 1.356 calculated using the Bishop simplified method. These results indicate that the finite element-based method used in this study effectively assesses slope stability problems.

The widespread K-L expansion is used to discretize the random field of the 2D log-normal distribution of the cohesion for computational efficiency. The accuracy of the random field discretization depends strongly on the number of terms in the eigenvalue expansion. Usually, increasing the number of terms improves accuracy. However, it also increases computational effort. A compromise between accuracy and computational cost is achieved by accepting a certain error level. Fig. 6 shows the decaying trend of the eigenvalues obtained by solving the integral eigenvalue problem; and Fig. 7 shows the eigenvectors corresponding to each eigenvalue, respectively. In this figure, the eigenvalues decay sharply with the number of K-L terms. In addition, the decay rate increases with increasing autocorrelation distance. In this paper, the accuracy rate 95% is used to determine the number of eigenvalue terms for the K-L expansion. The K-L expansion of 80 terms is a solution that achieves a balance between accuracy and efficiency when the horizontal and vertical autocorrelation distances are 20 and 2 m, respectively. When considering spatial variability, the size of the finite element is an important parameter that affects the accuracy of the reliability results. The element size of the random field is related to the correlation length of the autocorrelation function (Sudret and Der Kiureghian, 2000). Although finer meshes allow better estimation of the slope's safety factors and failure probabilities, the resulting computational time increases significantly. According to Jiang et al. (2014), this study used a 4-node quadrilateral mesh with a size of 0.5 m and a 3-node triangular mesh to balance precision and computational cost.

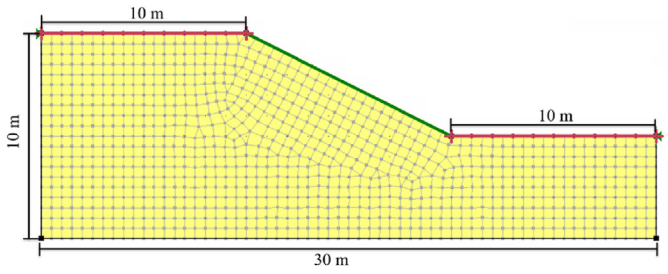

Fig. 5. Finite element model for slope in example 1.

Table 2
Material parameters in Example 1.

Parameter	Mean value	Coefficient of variation (COV)
Unit weight (kN/m^3)	20	Quantity is deterministic
Young's modulus (MPa)	100	Quantity is deterministic
Poisson's ratio	0.3	Quantity is deterministic
Cohesion (kPa)	23	0.3
Friction angle (°)		Quantity is deterministic

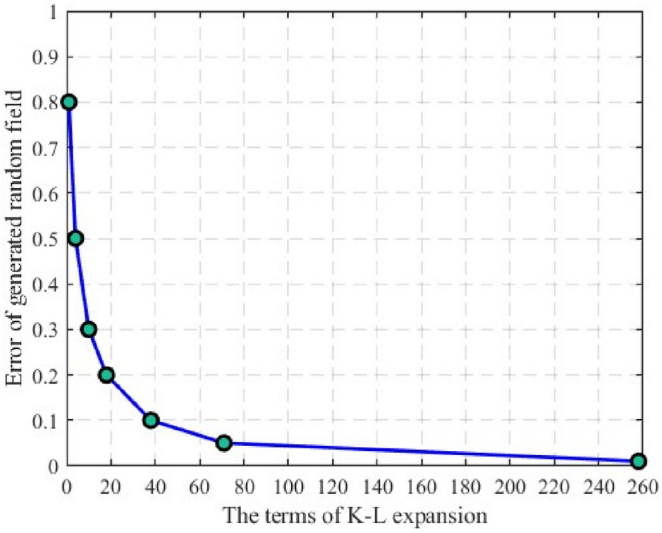

Fig. 6. The error of the K-L expansion.

Three main steps are performed to obtain a random field realization of the undrained shear strength with spatial variability. First, an independent standard normal sample matrix of dimension 80 × 900 is generated using LPSS. This is because 900 sets of random samples are sufficient for convergence for slope engineering with that failure probability. The 80-dimensional random variables of LPSS are generated by creating 40 groups of two random variables each. Then, the parameter matrix of the undrained shear strength in the physical space is obtained by K-L expansion. Finally, the sampled values of cohesion are assigned to each element separately. After deterministic analysis, the LPSS-MEDFM method was used to calculate the probability of failure of this slope engineering problem. Table 3 shows the failure probability results using the proposed approach for an undrained clay slope with an autocorrelation distance of $l_h = 20$ m and $l_v = 2$ m. In this table, some results from the literature are also shown for comparison. Among them, there are results obtained by LHS and MCS with MEDFM. For MCS-MEDFM and LHS-MEDFM, it requires 2000 and 1600 calculations, respectively. For LPSS-MEDFM, the results were calculated for 400, 900, 1600, 2500 and 3600 samples, respectively. It was found that only 900 deterministic calculations were needed to obtain reliable failure probability results. It is obvious that LPSS-MEDFM requires fewer deterministic analyses than LHS and MCS. These results indicate that the proposed approach can produce sufficiently accurate failure probability for smaller samples. The resulting PDF and CDF of f_s are shown in Figs. 8 and 9, respectively. The PDFs and CDFs calculated by the proposed approach in this paper are also consistent with Cho (2010), which shows that the proposed approach is efficient and trustworthy.

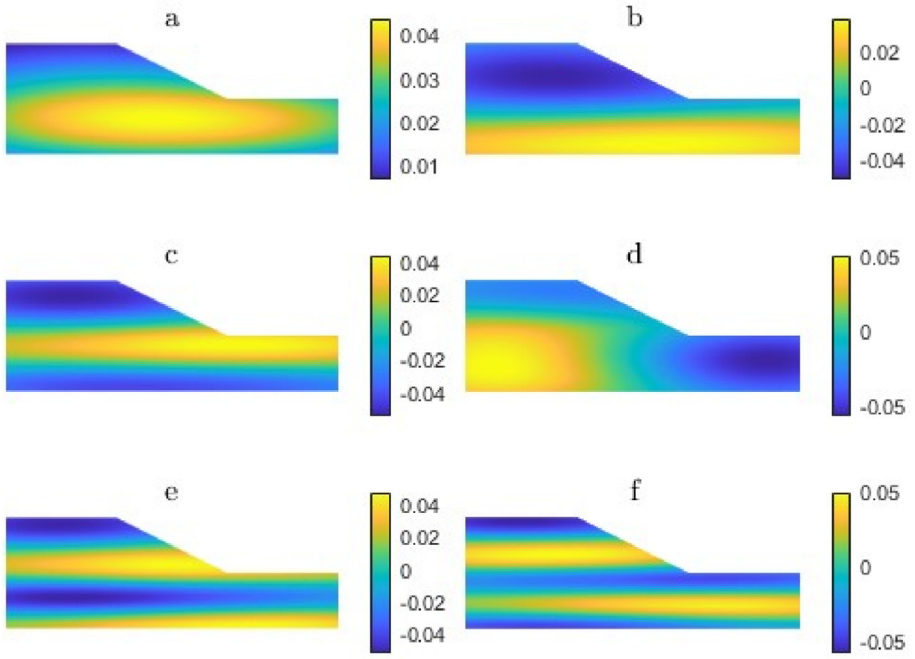

Fig. 7. Eigenfunctions of the autocorrelation function: (a) The first eigenfunction, (b) The second eigenfunction, (c) The third eigenfunction, (d) The fourth eigenfunction, (e) The fifth eigenfunction, and (f) The sixth eigenfunction.

To investigate the applicability of the method for small failure probabilities, we considered a scenario of undrained clay slope for a coefficient of variation of 0.15 (Jiang et al., 2015). The other parameters are the same as in the above case. The CDF results for this case are shown in Fig. 10. Table 4 shows the reliability results using the proposed approach for an undrained clay slope with a COV of 0.15. The result of the probability of failure calculated using the proposed approach in this paper is 1.5×10^{-4}. For this example, the results were calculated for 900, 1600, 2500, 3600, 4900 and 6400 samples, respectively. It was found that 3600 deterministic calculations were needed to obtain the failure probability results. This means that 3600 is the minimum number of samples to obtain accurate results, and the same results are obtained when the number of samples is larger than 3600. This is very close to the results in the literature. However, the sample size required by the method in this paper is significantly reduced compared to the literature (Liu et al., 2018). This result shows that the method is very effective for small failure probabilities. By comparing the results with those of integer order moments, it is found that the maximum entropy distribution with fractional order moments has apparent advantages for slopes with small failure probabilities considering spatial variability.

Table 3
Results in example 1 ($COV = 0.3$).

Deterministic analysis	Stochastic analysis	N_s	P_f	Source
LEM	LHS	1000	8.3×10^{-2}	Jiang et al. (2015)
LEM	MCS	100,000	7.6×10^{-2}	Cho (2010)
FEM	EQP + MRSM + MCS	10,000	7.4×10^{-2}	Liu et al. (2018)
FEM	MCS + MEDFM	2000	7.1×10^{-2}	This study
FEM	LHS + MEDFM	1600	7.2×10^{-2}	This study
FEM	LPSS + MEDIM	900	7.2×10^{-2}	This study
FEM	LPSS + MEDFM	900	7.4×10^{-2}	This study

Note: N_s is the number of deterministic finite element calculations performed, and its value in this paper is also the number of samples; LEM denotes the limit equilibrium method; MEDIM denotes the maximum entropy distribution with integer moments; EQP denotes the equivalent parameter; MRSM denotes the multiple response surface method.

4.2. Example 2: application to a c-φ slope

This example illustrates the applicability of the proposed approach to random fields with cross-correlation. Therefore, the same geometric model and computational conditions as in the first example are used, as shown in Fig. 5. The cohesion and friction angles are considered random fields with a log-normal distribution. Table 5 summarizes the statistical properties of the soil parameters for the slope considered. Young's modulus, Poisson's ratio, and the soil unit weight in this example are considered to be deterministic because their influence is relatively small compared to cohesion.

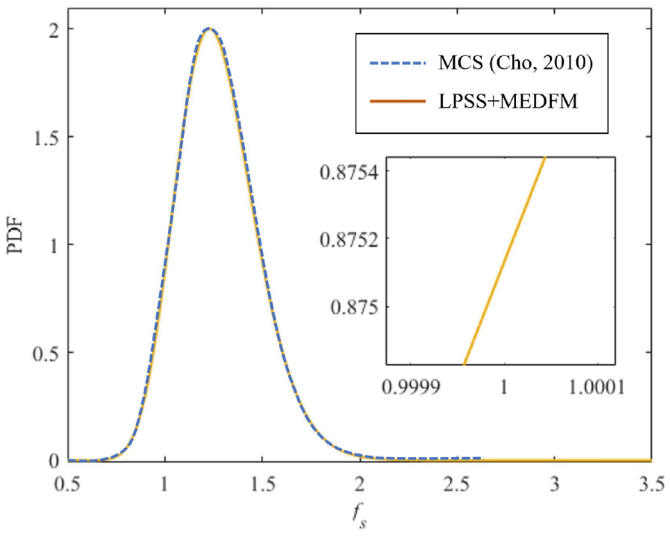

Fig. 8. PDF result in Example 1 ($COV = 0.3$).

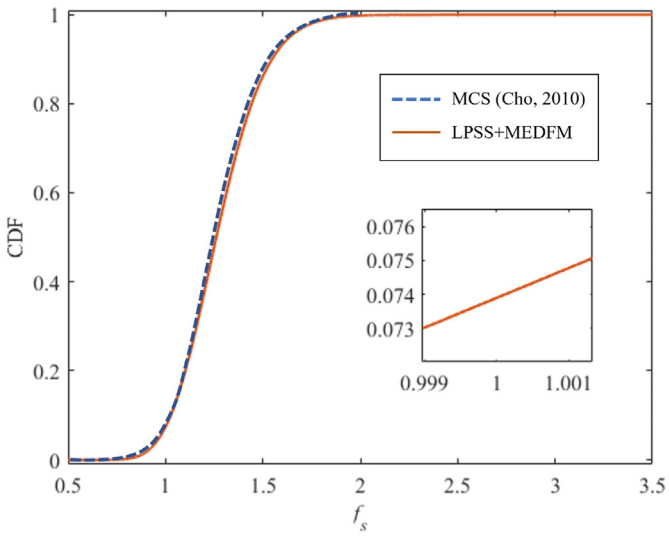

Fig. 9. CDF result in Example 1 ($COV = 0.3$).

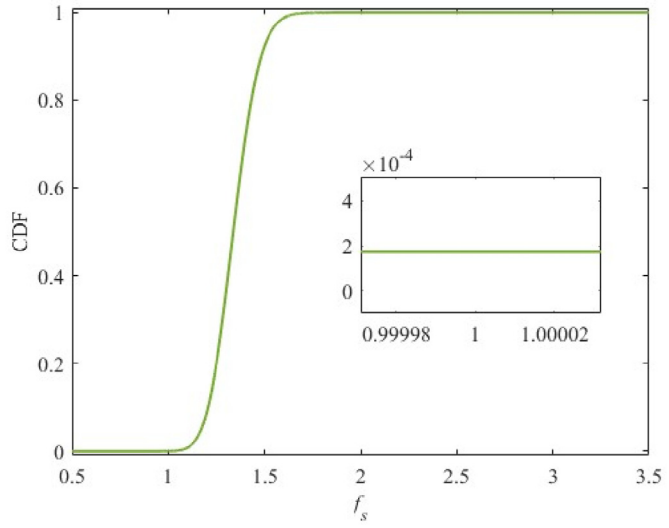

Fig. 10. CDF result in Example 1 ($COV = 0.15$).

The random field is first generated using the K-L method. Since we need to generate random fields separately for the cohesion and friction angle, we have a 160-dimensional random variable for this example. The generation of each random field is the same as in the first example. Then the method in Section 2.1 is used to generate the cross-correlated random fields. The realization of a random field of cohesion in this example is shown in Fig. 11.

Table 4
Results in example 1 ($COV = 0.15$).

Deterministic analysis	Stochastic analysis	N_s	P_f	Source
LEM	SRSM + RSSs + MCS	40,000	2.8×10^{-4}	Jiang et al. (2015)
FEM	EQP + LHS	40,000	1.25×10^{-4}	Liu et al. (2018)
FEM	EQP + MRSM + MCS	500,000	1.4×10^{-4}	Liu et al. (2018)
FEM	LPSS + MEDIM	3600	5.5×10^{-4}	This study
FEM	LPSS + MEDFM	3600	1.5×10^{-4}	This study

Note: SRSM denotes the stochastic response surfaces method; RSSs denotes the representative slip surfaces.

Table 5
Material parameters in Example 2.

Parameter	Mean value	Coefficient of variation (COV)
Unit weight (kN/m^3)	20	Quantity is deterministic
Young's modulus (MPa)	100	Quantity is deterministic
Poisson's ratio	0.3	Quantity is deterministic
Cohesion (kPa)	10	0.3
Friction angle (°)	20	0.2

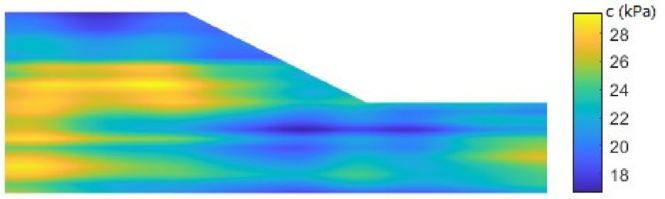

Fig. 11. The realization of the random field of cohesion in Example 2.

Table 6 shows the reliability results for a c-φ slope with an autocorrelation distance of $l_h = 25$ m and $l_v = 2.5$ m. The results in this example are shown in Figs. 12 and 13. The results of CDF for this case can be shown in Fig. 13. According to it, P_f of the slope can be obtained directly. The result of the probability of failure calculated using the approach proposed in this paper is 1.12×10^{-4}. Compared to Jiang et al. (2014), the results are of the same order of magnitude. The error can be accepted for slope engineering with a small failure probability. These results indicate that the proposed approach can produce sufficiently accurate failure probabilities.

Fig. 14 shows the results of calculating the reliability index for slopes with different cross-correlation coefficients using the proposed approach. The range of the cross-correlation coefficient is from −0.5 to 0.5. The reliability index of the slope decreases from 5.049 to 3.279. The results show that the cross-correlation coefficient has a considerable influence on the results of the probability of failure of the slope.

5. Discussion

This section provides a thorough discussion of the proposed approach in the paper. First, an application of the random field method in geotechnical engineering is discussed. Then the analysis of the proposed approach for calculating failure probability in geotechnical engineering is presented. Finally, the advantages and disadvantages of the proposed approach are compared with similar methods.

In the stochastic analysis of geotechnical engineering, the parameters of the random field are crucial. According to the results of this paper and existing studies, the mean value, COV, autocorrelation function and distance and cross-correlation coefficient may significantly influence the failure probability of geotechnical

Table 6
Results in example 2.

Deterministic analysis	Stochastic analysis	N_s	P_f	Source
FEM	2nd order PCE	462	6.26×10^{-4}	Jiang et al. (2014)
FEM	2nd order PCE	2500	4.32×10^{-4}	Jiang et al. (2014)
FEM	3rd order PCE	2500	3.55×10^{-4}	Jiang et al. (2014)
FEM	MCS	500,000	1.03×10^{-4}	This study
FEM	LPSS + MEDFM	3600	1.12×10^{-4}	This study

Note: PCE denotes the polynomial chaos expansion.

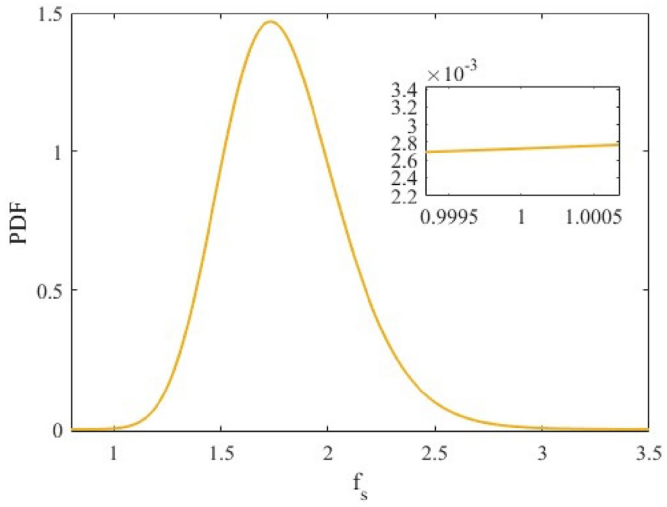

Fig. 12. PDF result in Example 2.

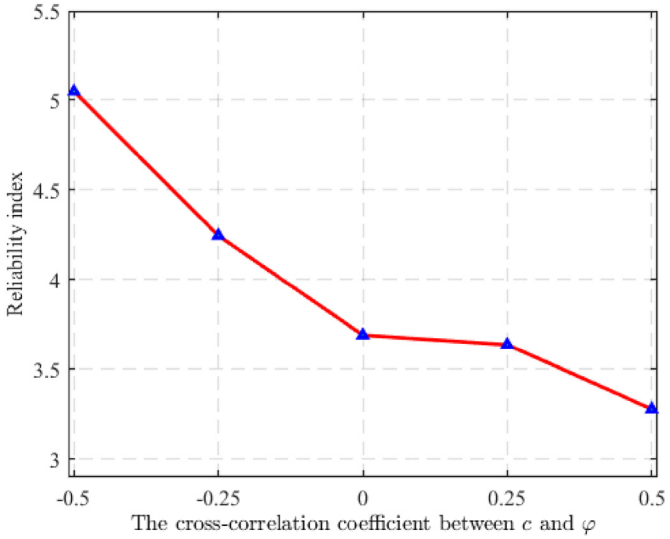

Fig. 14. The effect of the cross-correlation coefficient on the probability of failure.

engineering. While the topic holds significant importance, it must be noted that it is outside the scope of this paper.

Up to now, reliability methods have been developed rapidly. Nonetheless, the development has been less in geotechnical engineering reliability. Some of the reliability methods can be used in geotechnical engineering directly. However, geotechnical random field analysis has some unique characteristics, such as the complexity of materials, the large amount of single finite element calculations, and the high dimensionality of random variables. Therefore it is necessary to compare different methods to determine a better solution for geotechnical engineering needs. Through extensive literature research and calculations, it has been found that MEDFM is an excellent method for describing probability distributions. Unfortunately, it still requires a larger sample size when calculated with existing sampling methods such as MCS. So we investigated and calculated the existing sampling methods and found the advantages of the LPSS method and its ability to reduce the sample numbers significantly. Therefore, in this paper, an LPSS-MEDFM method is presented to solve the problem of calculating the failure probability of random fields in geotechnical engineering. In this method, the role of LPSS is to pull representative samples.

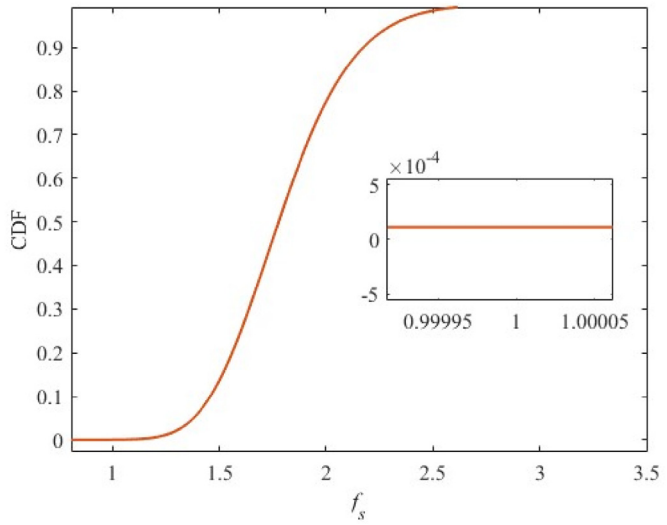

Fig. 13. CDF result in Example 2.

Specifically, LPSS generates samples using LSS after stratification, providing superior variance reduction when low-order interactions and main effects are present for many high-dimensional applications. The role of MEDFM is to describe the distribution of the sample, where the fractional moments are used to describe the statistical characteristics of the samples. LPSS and MEDFM must be coupled to be a complete and effective method, and it will not work without either part. It is emphasized that this combination takes advantage of the strengths of the different methods, the efficiency of which will be reduced without either. In example 1 of this paper, we have thoroughly compared the different methods. As shown, LPSS has a clear advantage over LHS and MCS due to the fewer samples required for reliable failure probability estimation.

The main advantage of the proposed approach is that it is efficient and steady compared with the existing reliability calculation methods for geotechnical random fields. In example 1 of this paper, for geotechnical engineering with a high failure probability ($>10^{-3}$), the number of finite element calculations required is 900. Compared with the existing literature, its computational efficiency has been significantly improved. Meanwhile, we compared the PDF and CDF of the safety factor with Cho (2010) and proved the method's accuracy. For geotechnical engineering with low failure probability ($<10^{-3}$), 3600 samples are required for our test case while we verify the accuracy of the results with MCS.

The approach presented in this paper is quite advantageous for dealing with geotechnical problems involving random fields, as it is possible to cope with high dimensional random variable spaces. However, this advantage may vanish in case that a particular problem involves a small number of random variables. For such cases, it may be more convenient to apply reliability methods based on surrogate models.

6. Conclusions

This work has presented an LPSS-MEDFM-based slope reliability analysis approach that accounts for the spatial variability of shear strength parameters. Log-normal random fields are considered for representing spatial variability, where the K-L expansion is implemented along a model for describing cross-autocorrelated random fields. The advantages of LPSS and its role in this study are then explained in detail. LPSS has a clear advantage relative to LHS for high-dimensional problems found when considering random

fields. Finally, the use of maximum entropy distribution to characterize complex distributions is described. We find that fractional moments can accurately analyze the statistical information of the data. Therefore, MEDFM was used to analyze the statistical information of the safety factor and to obtain the probability of failure of the slope. Two case studies were used as examples to demonstrate the capability and effectiveness of the presented approach for small failure probabilities. The presented approach is shown to provide a practical tool for calculating reliability problems even when complex finite element analysis is involved. The latter is due to the fact that the finite element analysis and probabilistic analysis are decoupled in this framework. Several conclusions can be drawn from this study:

(1) The proposed approach has high efficiency for geotechnical engineering problems with spatial variability. This is because the LPSS method has good efficiency and applicability for high-dimensional sampling problems compared to other methods. In fact, the random field models considered in this work comprise 80 and 160 random variables.
(2) The proposed approach is suitable for geotechnical engineering problems with a low probability of failure because the MEDFM method can obtain PDFs of safety factors from data with statistical information. This is because moments of fractional order include more information than moments of integer order. Combining fractional order moments with maximum entropy distribution makes the approach more efficient. For slope engineering with a high probability of failure, 900 samples are required, and for a very low probability of failure, only 1600 samples are needed.
(3) The coefficient of variation and cross-correlation coefficient of random fields significantly influence the failure probability of the slope. Failure probabilities may vary over orders of magnitude due to changes in them. Therefore, these parameters should be determined with careful consideration. The cross-correlation coefficient between cohesion and friction angle is generally negative and the resulting failure probability is much smaller than the case where they are independent. Thus, independent random fields should be generated when the cross-correlation coefficient between cohesion and friction angle is difficult to determine because it is a conservative scenario.

The presented approach has shown considerable potential for the problems considered in this work. However, due to their importance, the random field parameters of geotechnical engineering materials are required to be investigated in the future.

Declaration of competing interest

The authors declare that they have no known competing financial interests or personal relationships that could have appeared to influence the work reported in this paper.

Acknowledgments

We acknowledge the funding support from the China Scholarship Council (CSC).

References

Baecher, G.B., 2023. 2021 terzaghi lecture: geotechnical systems, uncertainty, and risk. J. Geotech. Geoenviron. Eng. 149, 03023001.
Cami, B., Javankhoshdel, S., Phoon, K.K., Ching, J., 2020. Scale of fluctuation for spatially varying soils: estimation methods and values. ASCE-ASME J RISK U A 6, 03120002.
Ching, J., Phoon, K.K., Stuedlein, A.W., Jaksa, M., 2019. Identification of sample path smoothness in soil spatial variability. Struct. Saf. 81, 101870.
Cho, S.E., 2010. Probabilistic assessment of slope stability that considers the spatial variability of soil properties. J. Geotech. Geoenviron. Eng. 136, 975–984.
Dai, H., Zheng, Z., Ma, H., 2019. An explicit method for simulating non-Gaussian and non-stationary stochastic processes by Karhunen-Loève and polynomial chaos expansion. Mech. Syst. Signal Process. 115, 1–13.
Deng, J., 2022. Probabilistic characterization of soil properties based on the maximum entropy method from fractional moments: model development, case study, and application. Reliab. Eng. Syst. Saf. 219, 108218.
Faes, M.G., Broggi, M., Spanos, P.D., Beer, M., 2022. Elucidating appealing features of differentiable auto-correlation functions: a study on the modified exponential kernel. Probabilist. Eng. Mech. 69, 103269.
Griffiths, D., Huang, J., Fenton, G.A., 2011. Probabilistic infinite slope analysis. Comput. Geotech. 38, 577–584.
Han, L., Wang, L., Zhang, W., Geng, B., Li, S., 2022. Rockhead profile simulation using an improved generation method of conditional random field. J. Rock Mech. Geotech. Eng. 14, 896–908.
Helton, J.C., Davis, F.J., 2003. Latin hypercube sampling and the propagation of uncertainty in analyses of complex systems. Reliab. Eng. Syst. Saf. 81, 23–69.
Jaynes, E.T., 1957. Information theory and statistical mechanics. Phys. Rev. 106, 620.
Ji, J., Zhang, C., Gao, Y., Kodikara, J., 2018. Effect of 2D spatial variability on slope reliability: a simplified FORM analysis. Geosci. Front. 9, 1631–1638.
Jiang, S.H., Huang, J., Griffiths, D., Deng, Z.P., 2022. Advances in reliability and risk analyses of slopes in spatially variable soils: a state-of-the-art review. Comput. Geotech. 141, 104498.
Jiang, S.H., Li, D.Q., Cao, Z.J., Zhou, C.B., Phoon, K.K., 2015. Efficient system reliability analysis of slope stability in spatially variable soils using Monte Carlo simulation. J. Geotech. Geoenviron. Eng. 141, 04014096.
Jiang, S.H., Li, D.Q., Zhang, L.M., Zhou, C.B., 2014. Slope reliability analysis considering spatially variable shear strength parameters using a non-intrusive stochastic finite element method. Eng. Geol. 168, 120–128.
Kapur, J.N., Kesavan, H.K., 1992. Entropy optimization principles and their applications. In: Entropy and Energy Dissipation in Water Resources. Springer, pp. 3–20.
Kumar, A., Tiwari, G., 2022. Jackknife based generalized resampling reliability approach for rock slopes and tunnels stability analyses with limited data: theory and applications. J. Rock Mech. Geotech. Eng. 14, 714–730.
Li, D.Q., Xiao, T., Cao, Z.J., Zhou, C.B., Zhang, L.M., 2016a. Enhancement of random finite element method in reliability analysis and risk assessment of soil slopes using subset simulation. Landslides 13, 293–303.
Li, P., Wang, Y., 2022. An active learning reliability analysis method using adaptive Bayesian compressive sensing and Monte Carlo simulation (ABCS-MCS). Reliab. Eng. Syst. Saf. 221, 108377.
Li, X., Zhang, L.M., Li, J., 2016b. Using conditioned random field to characterize the variability of geologic profiles. J. Geotech. Geoenviron. Eng. 142, 04015096.
Liu, L.L., Deng, Z.P., Zhang, S.h., Cheng, Y.M., 2018. Simplified framework for system reliability analysis of slopes in spatially variable soils. Eng. Geol. 239, 330–343.
Liu, P.L., Der Kiureghian, A., 1986. Multivariate distribution models with prescribed marginals and covariances. Probabilist. Eng. Mech. 1, 105–112.
Metropolis, N., Ulam, S., 1949. The Monte Carlo method. J. Am. Stat. Assoc. 44, 335–341.
Müller, J., Shoemaker, C.A., Piché, R., 2013. SO-MI: a surrogate model algorithm for computationally expensive nonlinear mixed-integer black-box global optimization problems. Comput. Oper. Res. 40, 1383–1400.
Pandey, M., 2002. An adaptive exponential model for extreme wind speed estimation. J. Wind Eng. Ind. Aerod. 90, 839–866.
Pandey, M., Gelder, P.v., Vrijling, J., 2001. Assessment of an L-kurtosis-based criterion for quantile estimation. J. Hydraul. Eng. 6, 284–292.
Phoon, K.K., Kulhawy, F.H., 1999. Characterization of geotechnical variability. Can. Geotech. J. 36, 612–624.
Rubinstein, R.Y., Kroese, D.P., 2016. Simulation and the Monte Carlo Method. John Wiley & Sons.
Salgado, R., Kim, D., 2014. Reliability analysis of load and resistance factor design of slopes. J. Geotech. Geoenviron. Eng. 140, 57–73.
Santamarina, J., Altschaeffl, A., Chameau, J., 1992. Reliability of slopes: incorporating qualitative information (abridgment). Transport. Res. 1343, 1–5.
Sepúlveda-García, J.J., Alvarez, D.A., 2022. On the use of copulas in geotechnical engineering: a tutorial and state-of-the-artreview. Arch. Comput. Methods Eng. 1–51.
Shi, Y., Lu, Z., Li, Z., Wu, M., 2018. Cross-covariance based global dynamic sensitivity analysis. Mech. Syst. Signal Process. 100, 846–862.
Shields, M.D., 2016. Refined latinized stratified sampling: a robust sequential sample size extension methodology for highdimensional Latin hypercube and stratified designs. Int. J. Uncertain. Quantification 6.
Shields, M.D., Zhang, J., 2016. The generalization of Latin hypercube sampling. Reliab. Eng. Syst. Saf. 148, 96–108.
Spanos, P.D., Beer, M., Red-Horse, J., 2007. Karhunen–Loève expansion of stochastic processes with a modified exponential covariance kernel. J. Eng. Mech. 133, 773–779.
Sudret, B., Der Kiureghian, A., 2000. Stochastic Finite Element Methods and Reliability: a State-Of-The-Art Report. Department of Civil and Environmental Engineering, University of California, Berkeley.
Tagliani, A., 1999. Hausdorff moment problem and maximum entropy: a unified approach. Appl. Math. Comput. 105, 291–305.

Vořechovskỳ, M., 2008. Simulation of simply cross correlated random fields by series expansion methods. Struct. Saf. 30, 337–363.
Wang, B., Liu, L., Li, Y., Jiang, Q., 2020. Reliability analysis of slopes considering spatial variability of soil properties based on efficiently identified representative slip surfaces. J. Rock Mech. Geotech. Eng. 12, 642–655.
Wang, Y., Cao, Z., Au, S.K., 2011. Practical reliability analysis of slope stability by advanced Monte Carlo simulations in a spreadsheet. Can. Geotech. J. 48, 162–172.
Wang, Y., Cao, Z., Li, D., 2016. Bayesian perspective on geotechnical variability and site characterization. Eng. Geol. 203, 117–125.
Wang, Z.Z., Jiang, S.H., 2023. Characterizing geotechnical site investigation data: a comparative study using a novel distribution model. Acta Geotech 18, 1821–1839.
Whitley, D., 1994. A genetic algorithm tutorial. Stat. Comput. 4, 65–85.
Winterstein, S.R., Kashef, T., 2000. Moment-based load and response models with wind engineering applications. J. Sol. Energy Eng. 122, 122–128.
Xu, J., Dang, C., 2019. A novel fractional moments-based maximum entropy method for high-dimensional reliability analysis. Appl. Math. Model. 75, 749–768.
Zhang, X., Liu, J., Yan, Y., Pandey, M., 2019. An effective approach for reliability-based sensitivity analysis with the principle of maximum entropy and fractional moments. Entropy 21, 649.
Zhang, X., Low, Y.M., Koh, C.G., 2020. Maximum entropy distribution with fractional moments for reliability analysis. Struct. Saf. 83, 101904.
Zhang, X., Pandey, M.D., 2013. Structural reliability analysis based on the concepts of entropy, fractional moment and dimensional reduction method. Struct. Saf. 43, 28–40.
Zhao, T., Wang, Y., 2020. Non-parametric simulation of non-stationary non-Gaussian 3D random field samples directly from sparse measurements using signal decomposition and Markov chain Monte Carlo (MCMC) simulation. Reliab. Eng. Syst. Saf. 203, 107087.

Chengxin Feng is currently a PhD student at Leibniz University Hannover, Germany. He obtained his BSc and MSc degrees in hydraulic engineering from the China Three Gorges University in 2018 and 2021, respectively. His research interests include geotechnical uncertainty analysis, reliability analysis, and interval analysis.